Impact of nonequilibrium phonons on the electron dynamics in terahertz quantum cascade lasers

Rita Claudia Iotti,[1,a)] Fausto Rossi,[1] Miriam Serena Vitiello,[2] Gaetano Scamarcio,[2] Lukas Mahler,[3] and Alessandro Tredicucci[3]
[1]*Dipartimento di Fisica, Politecnico di Torino, Corso Duca degli Abruzzi 24, 10129 Torino, Italy*
[2]*CNR-Istituto di Fotonica e Nanotecnologie and Departimento di Fisica, Università di Bari "Aldo Moro", Via Amendola 173, 70126 Bari, Italy*
[3]*NEST CNR-INFM and Scuola Normale Superiore, Piazza dei Cavalieri 7, 56126 Pisa, Italy*

(Received 21 April 2010; accepted 28 June 2010; published online 21 July 2010)

In this paper we investigate, both theoretically and experimentally, nonequilibrium electron and phonon effects in quantum-cascade devices. In particular, we have developed a Monte Carlo-based global kinetic approach describing the complete interacting electronic subsystem (i.e., the full set of active-region and injector subbands) coupled to out-of-equilibrium longitudinal polar-optical (LO) phonons, which in turn will decay anharmonically into thermalized acoustic modes. Simulated results obtained for a prototypical terahertz emitting device show a very good agreement with measured data, evidencing how the nonequilibrium LO phonon population affects the electro-optical device performances. The latter may be qualitatively reproduced in terms of a global effective temperature of the heated phononic system. © *2010 American Institute of Physics*. [doi:10.1063/1.3464977]

Quantum-cascade lasers (QCLs) are unipolar semiconductor-based nanostructured devices representing, at present, one of the most relevant achievements of the band gap engineering technological potential. Indeed, the impressive and rapid development, both in design and fabrication, that QCLs have undergone since their first demonstration in 1994,[1] makes them an extremely reliable and versatile coherent light source in the whole mid- to far-infrared spectral range.

The principle of operation of QCLs exploits downhill electronic transitions along the biased, suitably designed ladder of subbands in which the heterostructure conduction band is split due to quantum confinement. In particular, the gain regime in the active region is established and maintained by means of a properly tailored electron energy relaxation dynamics, resulting in a selective depopulation of the diverse subband states.

While such a tailoring is generally far from intuitive in far-infrared (terahertz, THz) emitters, where a complex and sinergistic interplay between the various nonradiative energy relaxation/dephasing channels (carrier-phonon, carrier-carrier, . . ., etc.) might take place,[2] it can be more easily pictured out in mid-infrared sources, where the photon energy is larger than the longitudinal polar-optical (LO) phonon one.

In conventional mid-IR, as well as in THz resonant-phonon designs, the separation between the lower laser- and the ground-subband matches the LO phonon energy so to maximize carrier relaxation out of the former into the latter via LO-phonon emission. In this case, a significant nonequilibrium ("hot")[3] population of LO phonons is present in the active region of the operating device when, as it is generally the case, their generation rate is larger than the anharmonic decay rate into acoustic modes.

The impact of hot-phonon effects on the electron relaxation dynamics, and therefore, on the performances of QCLs, has been theoretically addressed in the past, in terms of Monte Carlo (MC) kinetic treatments either limited to a subset of subbands[4–6] or within a prototypical Krönig–Penney model.[5,6] Recent experimental studies have pointed out distinctive nonequilibrium phonon features both in mid-IR (Ref. 7) as well as in THz QCLs,[8,9] evidencing a significant heating of both the electron and lattice systems.[10] Aim of this paper is to provide a *global* kinetic theoretical description of these effects in realistic QCL designs.

Within the semiclassical framework, the investigation of the interacting electron-phonon system should include both the electron and the phonon coupled Boltzmann equations. This task is quite demanding, since it would require, for the latter, the inclusion of both acoustic and optical modes, preferably with finite size and quantization effects. To start focusing on the main physical aspects of the energy redistribution between charge carriers and lattice degrees of freedom, in this work we consider the full electron subsystem (i.e., the complete set of active-region and injector subbands) interacting with bulk LO-phonon modes, whose decay into acoustic (lattice thermal bath) modes is accounted for by means of a phenomenological lifetime τ.

In particular, within the Fermi's golden rule approximation, the LO-phonon interaction translates into the following term in the electronic Boltzmann transport equation for the distribution function $f_{\nu\mathbf{k}}$ (of the single-particle state in subband ν and with wave vector $\mathbf{k}$):

$$\left.\frac{d}{dt}f_{\nu\mathbf{k}}\right|_{\text{e-LO}} = \sum_{\mathbf{q}^{\pm}}\left(\mathcal{N}_{\mathbf{q}}+\frac{1}{2}\pm\frac{1}{2}\right) \sum_{\nu'\mathbf{k}'}\left[(1-f_{\nu\mathbf{k}})P^{\mathbf{q}^{\pm}}_{\nu\mathbf{k},\nu'\mathbf{k}'}f_{\nu'\mathbf{k}'} - (1-f_{\nu'\mathbf{k}'})P^{\mathbf{q}^{\pm}}_{\nu'\mathbf{k}',\nu\mathbf{k}}f_{\nu\mathbf{k}}\right], \quad (1)$$

a)Electronic mail: rita.iotti@polito.it.

where $\mathcal{N}_{\mathbf{q}}$ is the phonon population of the LO-mode with wave vector $\mathbf{q}$, $P^{\mathbf{q}\pm}_{\nu\mathbf{k},\nu'\mathbf{k}'}=(2\pi/\hbar)|g^{\pm}_{\nu\mathbf{k},\nu'\mathbf{k}';\mathbf{q}}|^2\delta(\varepsilon_{\nu\mathbf{k}}-\varepsilon_{\nu'\mathbf{k}'}\pm\varepsilon_{\mathbf{q}})$, where $g^{\pm}_{\nu\mathbf{k},\nu'\mathbf{k}';\mathbf{q}}$ is the Frölich carrier-phonon coupling coefficient, and the sign +(−) refers to emission (absorption) processes.

To properly model the carrier-phonon interacting systems, the Boltzmann transport equation for the electron subsystem, with the contribution in Eq. (1), goes together with the following phonon counterpart:

$$\frac{d}{dt}\mathcal{N}_{\mathbf{q}}=\sum_{\pm}\pm\left(\mathcal{N}_{\mathbf{q}}+\frac{1}{2}\pm\frac{1}{2}\right)\sum_{\nu\mathbf{k}\neq\nu'\mathbf{k}'}(1-f_{\nu\mathbf{k}})P^{\mathbf{q}\pm}_{\nu\mathbf{k},\nu'\mathbf{k}'}f_{\nu'\mathbf{k}'}-\frac{\mathcal{N}_{\mathbf{q}}-\mathcal{N}^{\mathrm{th}}_{\mathbf{q}}}{\tau}, \tag{2}$$

where the $-(\mathcal{N}_{\mathbf{q}}-\mathcal{N}^{\mathrm{th}}_{\mathbf{q}})/\tau$ term accounts for loss processes due to anharmonic decay into acoustic modes, $\mathcal{N}^{\mathrm{th}}_{\mathbf{q}}$ being the Bose–Einstein distribution at the lattice temperature T_L.

The main advantage of treating the carrier-phonon system via such a coupled-equation formalism is that, due to their structure, the latter may be conveniently sampled by means of a generalized MC simulation able to deal with a variable number of phonons, and therefore, implemented in state-of-the-art simulation tools.[11,12] In particular, the use of a periodic boundary condition approach allows us to evaluate device performances in a 'closed-circuit' scheme, in which the only free parameters are the LO-phonon lifetime τ and the lattice temperature T_L. The latter may be accessed by means of state-of-the-art microprobe band-to-band photoluminescence experiments,[9,10,13] while realistic values for the former in bulk materials are in the range 6–9 ps.[14]

We have applied the above simulation scheme to a resonant phonon THz QCL device based on the quantum design described in Ref. 15; the active region includes 200 periods and has been embedded between two highly doped (5×10^{18} cm^{-3}) GaAs layers and fabricated on a double metal optical waveguide. Besides carrier-LO phonon scattering, we have included also carrier-carrier interaction in the electron dynamical equation, employing the well-established time-dependent static-screening model commonly adopted in two-dimensional systems.[16] The lifetime τ is set to 6 ps.

Figure 1 shows the simulated current-voltage characteristics of our prototypical device. Here, the current density as a function of the applied voltage has the typical behavior of QCL structures, i.e., it increases on increasing the bias as long as the injector and upper laser subbands are kept aligned, while a negative differential resistance region shows up at higher fields. Measured data are also reported in the same figure. In particular, the experimental values of the electric field have been estimated by subtracting a parasitic drop of 5 V at the Schottky barrier from the measured voltage values. Moreover, for the sake of comparison with theoretical findings and since what is actually experimentally accessible is the total current, the measured results have been divided by an effective surface. The latter is estimated by matching the two sets of data safely well into the lasing regime, that is around 10.5 kV/cm, and amounts to 2.2×10^{-4} cm^2. This value is in reasonable agreement with the device dimensions; however, an accurate estimate of the experimental value of the effective area is obscured by the uncertainties in the definition of the surface in which the current is really flowing in our setup.

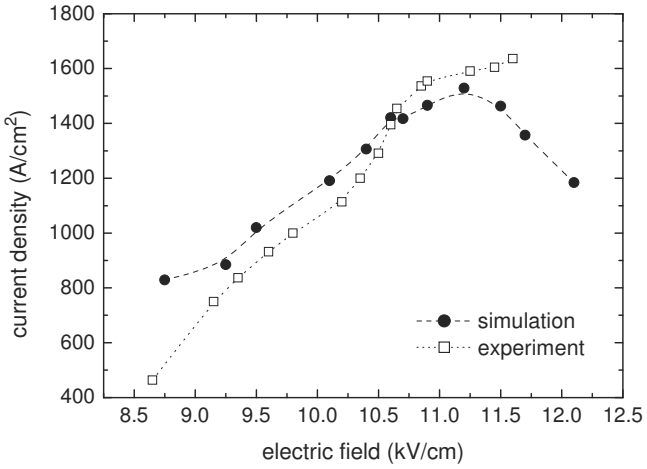

FIG. 1. Simulated (disks) and measured (squares) current density as a function of the applied electric field. Experimental values for the latter have been estimated by subtracting a parasitic drop of 5 V at the Schottky barrier from the measured voltage. Experimental current data have been divided by an effective surface to compare with theoretical results. Lines are a guide to the eye.

The agreement between the simulated and the observed current-voltage trend is extremely good.[17] A further analysis shows that this is the result of both nonequilibrium LO-phonon population, as confirmed by MC-like results for a similar QCL structure,[18] and Joule heating of the device. More specifically, in Fig. 2 we compare the above discussed theoretical results (disks) with those (triangles) of a simulation performed with an equilibrium LO-phonon distribution at the cryostat temperature (80 K). The latter, besides being significantly lower, show a milder slope. The Joule effect seems to be responsible for most of the trend observed in Fig. 1. Indeed, this can be inferred by comparing the above data with the results (empty squares) of a simulation performed with an LO phonon subsystem in equilibrium at the *measured* lattice temperature T_L (which varies with the applied bias, as shown in Fig. 3): while the absolute values in this latter case are slightly lower than those of Fig. 1, the trend is basically reproduced.

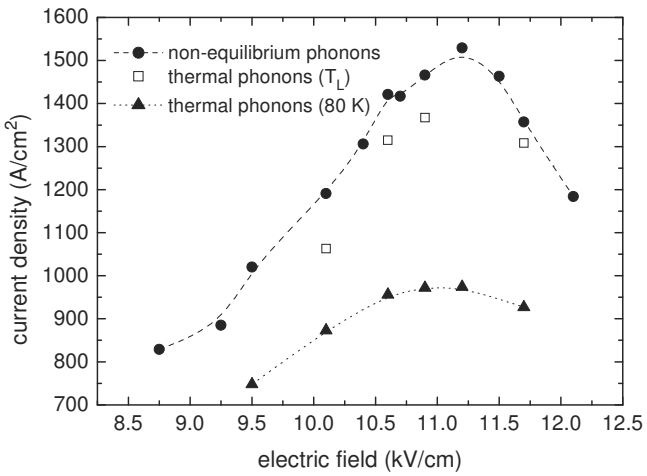

FIG. 2. Simulated current density vs applied field characteristics, obtained under diverse conditions for the LO-phonon subsystem: equilibrium at the cryostat temperature (triangles), equilibrium at the measured lattice temperature T_L (empty squares), nonequilibrium (disks, same data of Fig. 1).

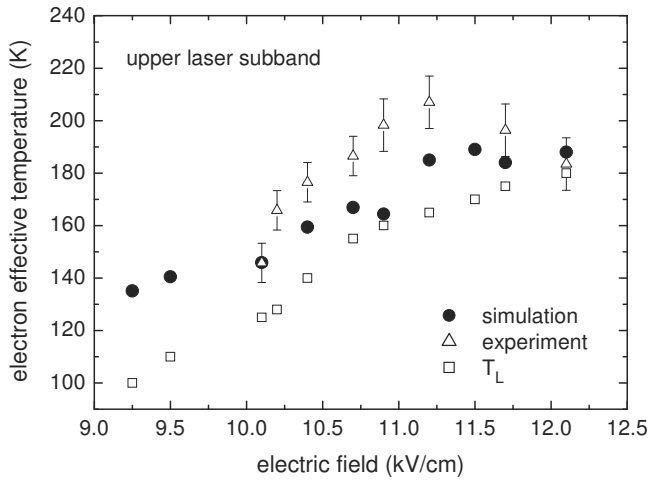

FIG. 3. Simulated (disks) and measured (triangles) electron effective temperature for the upper laser subband, as a function of the applied electric field. The lattice temperature T_L is also shown (squares).

As far as the optical gain regime is concerned, an unavoidable drawback of the resonant-phonon design is that the nonequilibrium LO-phonon distribution might produce a detrimental effect, diminishing the electron cooling rates out of the lower laser subband. This is confirmed by our simulated experiments, where we found a 15% reduction in the population inversion, with respect to the ideal case in which the electron subsystem is interacting with a lattice thermal bath at the cryostat temperature.

A relevant key feature of the present kinetic approach is that it allows us to directly access the carrier distribution functions of the diverse device subbands, as a pure output of our Monte Carlo simulation. In other words, no hypothesis of intrasubband thermalization is a-priori made. The latter, instead, may eventually show up due to the sinergistic interplay between carrier-carrier and carrier-LO phonon scattering. This is indeed the case also of the device we are considering, where the simulated distribution functions for the various subbands present a typical heated Maxwellian form. In particular, Fig. 3 reports the estimated electron effective temperature in the upper laser subband (disks) as a function of the applied bias. Theoretical data are in very good agreement with experimental results (triangles) obtained via microprobe band-to- band photoluminescence. Figure 3 also shows the lattice temperature T_L adopted in the MC simulation (squares), inferred from the same experimental technique: The 'hot electron' regime, in which the charge carriers' temperature is higher than the lattice one, is then evident.

To conclude, in this paper we have investigated, both theoretically and experimentally, hot electron-hot phonon effects in a prototypical THz QCL structure. In particular, we have developed an MC-based global kinetic approach describing the complete interacting electronic subsystem (i.e., the complete set of active-region and injector subbands), coupled to a bulk LO-phonon subsystem, whose decay into acoustic modes is modeled by a phenomenological lifetime. Simulated results show a very good agreement with experimental data, evidencing how the nonequilibrium phonon population may affect the electro-optical device performances.

[1]J. Faist, F. Capasso, D. L. Sivco, C. Sirtori, A. L. Hutchinson, and A. Y. Cho, Science **264**, 553 (1994).
[2]R. Köhler, R. C. Iotti, A. Tredicucci, and F. Rossi, Appl. Phys. Lett. **79**, 3920 (2001).
[3]It might be useful to stress that, while the term "hot" may suggest a thermalized Bose-type form of the nonequilibrium phonon distribution, this is usually not the case. The same applies to the electron distribution function as well.
[4]G. Paulavičius, V. Mitin, and M. A. Stroscio, J. Appl. Phys. **84**, 3459 (1998).
[5]F. Compagnone, M. Manenti, A. Di Carlo, and P. Lugli, Physica B **314**, 336 (2002).
[6]C. Jirauschek and P. Lugli, J. Comput. Electron. **7**, 436 (2008).
[7]V. Spagnolo, G. Scamarcio, M. Troccoli, F. Capasso, C. Gmachl, A. M. Sergent, A. L. Hutchinson, D. L. Sivco, and A. Y. Cho, Appl. Phys. Lett. **80**, 4303 (2002).
[8]V. Spagnolo, M. S. Vitiello, G. Scamarcio, B. S. Williams, S. Kumar, Q. Hu, and J. L. Reno, J. Phys.: Conf. Ser. **92**, 012018 (2007).
[9]G. Scamarcio, M. S. Vitiello, V. Spagnolo, S. Kumar, B. Williams, and Q. Hu, Physica E (Amsterdam) **40**, 1780 (2008).
[10]M. S. Vitiello, G. Scamarcio, V. Spagnolo, B. S. Williams, S. Kumar, Q. Hu, and J. L. Reno, Appl. Phys. Lett. **86**, 111115 (2005).
[11]R. C. Iotti and F. Rossi, Phys. Rev. Lett. **87**, 146603 (2001).
[12]R. C. Iotti and F. Rossi, Rep. Prog. Phys. **68**, 2533 (2005).
[13]M. S. Vitiello, G. Scamarcio, V. Spagnolo, J. Alton, S. Barbieri, C. Worral, H. E. Beere, D. A. Ritchie, and C. Sirtori, Appl. Phys. Lett. **89**, 021111 (2006).
[14]J. Shah, *Ultrafast Spectroscopy of Semiconductors and Semiconductor Nanostructures* (Springer, Berlin, 1998).
[15]S. Kumar, B. S. Williams, S. Kohen, Q. Hu, and J. L. Reno, Appl. Phys. Lett. **84**, 2494 (2004).
[16]S. M. Goodnick and P. Lugli, Phys. Rev. B **37**, 2578 (1988).
[17]Scattering mechanisms not included in our model-like, e.g., interface roughness and carrier impurity scattering may affect the transport properties of real devices and have to be considered if one is interested in a strictly quantitative analysis. Such processes, however, do not significantly modify the trend of the current-voltage characteristics since, opposite to carrier-LO phonon scattering, they are threshold-less mechanisms, and therefore, poorly dependent on the applied bias. They are, moreover, strongly device dependent and do not represent by themselves an energy dissipation channel.
[18]J. T. Lü and C. Cao, Appl. Phys. Lett. **88**, 061119 (2006).